2013

The Jormungand Climate Model

Christopher V. Rackauckas
Oberlin College

The Jormungand Climate Model

By Christopher V. Rackauckas

Abstract

The geological and paleomagnetic record indicate that around 750 million and 580 millions years ago glaciers grew near the equator, though as of yet we do not fully understand the nature of these glaciations. The well-known Snowball Earth Hypothesis states that the Earth was covered entirely by glaciers. However, it is hard for this hypothesis to account for certain aspects of the biological evidence such as the survival of photosynthetic eukaryotes. Thus the Jormungand Hypothesis was developed as an alternative to the Snowball Earth Hypothesis. In this paper we investigate previous models of the Jormungand state and look at the dynamics of the Hadley cells to develop a new model to represent the Jormungand Hypothesis. We end by solving for an analytical approximation to the model using a finite Legendre expansion and geometric singular perturbation theory. The resultant model gives a stable equilibrium point near the equator with strong hysteresis that satisfies the Jormungand Hypothesis.

1 Introduction

Geological and paleomagnetic evidence indicates that glaciers grew near the equator during at least two time periods between 750 million and 580 million years ago in what is known as the Neoproterozoic era [3, 4]. To explain these findings, the Snowball Earth Hypothesis was proposed. The Snowball Earth hypothesis states the the Earth's surface was covered entirely by glaciers. However, biological evidence such as the survival of photosynthetic eukaryotes has lead some researchers to support alternative hypotheses [1]. Many of these alternatives are unable to satisfy the strong hysteresis of CO_2 seen in the data (which is the existence of two stable states over a large range of CO_2 values). One alternative which has shown promise in its ability to show strong hysteresis is the Jormungand Hypothesis. The Jormungand Hypothesis agrees with the Snowball Earth Hypothesis about the existance of a large glaciation but disagrees about the exact nature of this glaciation near the equator. The Jormungand Hypothesis instead asserts that the ice sheets near the equator were devoid of snow cover and that there was a belt of open water. The purpose of this paper is to present and augment the models which are used to understand these large glaciations.

The paper is outlined as follows. Section 2 will introduce the models and walk through previous research that has been done with the models. Section 3 will introduce a new version of the model which will then be analyzed. Section 4 will give concluding remarks.

2 The Budyko-Widiasih Model

2.1 Introduction to the Budyko-Widiasih Model

The models in this paper are what are known as Energy Balance Models (EBMs), which are conceptual lower-order models used to show the general interactions between important system variables [9]. They focus on the Earth's "energy diet," relating the important factors that cause energy to enter, exit, and

flow through the Earth's system. Due to the simplicity of these models, one can more readily extrapolate important information about the relations between system variables. This is not to be confused with the General Circulation Models (GCMs) which include a multitude of scientific processes and are analyzed computationally to understand the Earth's system.

We wish to model the Earth's ice-albedo feedback system. The albedo of an object is the percentage of incident light that it reflects. It is known that the albedo of ice is higher than the albedo of land and water, which in turn decreases the insolation (incoming solar radiation) that is absorbed by the Earth's system in areas covered in glaciers.

To model this system, our variable of interest is the annual mean surface temperature $T = T(y,t)$ as a function of latitude and time. The spatial variable is denoted by y which is the sine of the latitude. Note that by writing y in this manner, $y \in [-1,1]$ where -1 is the South Pole and 1 is the North Pole. We will assume that the Earth is symmetric about the equator and thus take $y \in [0,1]$. Thus the Budyko model can be written as follows [6]:

$$R\frac{\partial T}{\partial t} = E_{in} - E_{out} - M. \tag{2.1}$$

The parameter R is known as the heat capacity of the Earth's system which we will approximate to be the constant $R = 4 \times 10^8 \frac{J/m^2}{^\circ C}$ [8]. The term E_{in} can be expressed by the formula

$$E_{in} = \text{Solar Insolation} \times \text{ Absorption Percentage} = Qs(y)(1 - \alpha(y,\eta)). \tag{2.2}$$

The parameter $Q = 343\,W/m^2$ is the global average insolation. The function $s = s(y)$ is the distribution of insolation as a function of latitude. The function s satisfies the normalization requirement

$$\int_0^1 s(y)dy = 1. \tag{2.3}$$

North pointed out that s is uniformly approximated to within 2% by the quadratic function $s(y) = 1.241 - .0723y^2$ [13]. We will use this approximation for the rest of the paper. Recall that the albedo α describes the percentage of the Sun's energy reflected by the Earth. We define the variable η to be the ice line, the furthest extent of the Earth's glaciers. Given the relation between albedo and the presence of glaciers on the Earth's surface, we let $\alpha = \alpha(y,\eta)$. The Budyko model takes the albedo function to be defined by the Budyko Albedo Function

$$\alpha(y,\eta) = \begin{cases} \alpha_s & y > \eta \\ \frac{1}{2}(\alpha_s + \alpha_w) & y = \eta \\ \alpha_w & y < \eta \end{cases}. \tag{2.4}$$

This function simply states that the albedo is that of snow covered ice $\alpha_s = .62$ above the ice line and that of water $\alpha_w = .32$ below the ice line (where $\alpha_s > \alpha_w$). The process through which the Earth radiates energy is complicated by the Earth's atmosphere. The Budyko model uses a linear approximation for the outgoing radiation

$$E_{out} = A + BT, \tag{2.5}$$

where $A = 202\,W/m^2$ and $B = 1.9\,\frac{W/m^2}{^\circ C}$ are determined by satellite data. The last part of the Budyko model describes the transport of energy between latitudes, also known as the meridional heat transport. This process is complex and involves winds and ocean currents but its effects can be approximated by a

simple linear relation to the mean[1]. We define $\overline{T}$ as the mean Earth temperature:

$$\bar{T} = \int_0^1 T(y,t)dy, \tag{2.6}$$

and define the meridional heat transport as

$$M = C(T - \bar{T}), \tag{2.7}$$

where the parameter $C = 3.04 \frac{W/m^2}{^\circ C}$ is determined from data.

As stated, the model describes how the termperature distributions change over time for a constant ice line η. However, we would expect that the ice line would be variable since warmer temperatures should melt the glaciers while cooler temperatures should cause the glaciers to grow. The ice line dynamics are introduced into this model by Widiasih's Ice Line Condition [8] which models the change in the ice line as a function of the temperature at the ice line

$$\frac{d\eta}{dt} = \epsilon(T(\eta,\eta) - T_c), \tag{2.8}$$

where $\epsilon > 0$. $T(\eta,\eta)$ is defined as the average of the temperatures just above and just below the ice line, or more rigorously

$$T(\eta,\eta) = \frac{1}{2}(\lim_{y\to\eta^-} T(y,t) + \lim_{y\to\eta^+} T(y,t)). \tag{2.9}$$

The constant $T_c = -10^\circ C$ denotes the critical temperature for melting glaciers and is based on observations of the modern climate [1]. Thus this condition simply states the the ice line increases toward the pole if the temperature at the ice line is high enough to melt glaciers and that the ice line grows towards the equator if the temperature at the ice line is lower than the temperature to melt glaciers.

Thus the Budyko-Widiasih model's defining equations are

$$\begin{aligned} R\frac{\partial T}{\partial t} &= Qs(y)(1-\alpha(y,\eta)) - (A+BT) - C(T-\overline{T}), \\ \frac{\partial \eta}{\partial t} &= \epsilon(T(\eta,\eta) - T_c). \end{aligned} \tag{2.10}$$

2.2 Previous Research on the Budyko-Widiasih Model

The Budyko-Widiasih model is used to try to understand the behavior of $(T(y,\eta),\eta)$ pairs over time. Denote the equilibrium temperature distribution $T^*(y,\eta)$ to be the distribution for a constant ice line η (i.e. $\epsilon = 0$) that satisfies

$$R\frac{\partial T^*}{\partial t} = Qs(y)(1-\alpha(y,\eta)) - (A+BT^*) - C(T^* - \overline{T^*}) = 0. \tag{2.11}$$

We can solve for the average global annual temperature for a constant ice line as

$$\overline{T^*}(\eta) = \int_0^1 T^*(y,\eta)dy = \frac{1}{B}(Q(1-\bar{\alpha}(\eta) - A) \tag{2.12}$$

[1]This approximation can also be expressed by the assumption that all latitudes of the Earth are sufficiently "close" for heat transport or that heat can transport sufficiently quickly to any given latitude. This would imply that the entirety of the Earth is the "environment" for a given latitude and thus Newton's Law of Cooling would result in a relaxation towards the mean.

where

$$\bar{\alpha}(\eta) = \int_0^1 s(y)\alpha(y,\eta)dy. \tag{2.13}$$

Thus we can solve for the annual surface temperature at equilibrium to be

$$T^*(y,\eta) = \frac{1}{B+C}(Qs(y)(1-\alpha(y,\eta)) - A + C\overline{T^*}) = \frac{Q}{B+C}\left(s(y)(1-\alpha(y,\eta)) + \frac{C}{B}(1-\bar{\alpha}(\eta))\right) - \frac{A}{B}. \tag{2.14}$$

It is generally assumed that over time the temperature distributions T converge towards the equilibrium temperature distributions T^*. Thus for ϵ sufficiently small, the temperature distributions functions will approximately be the equilibrium temperature distribution functions for a given η. Let h be the function that satisfies the relation

$$\frac{\partial \eta}{\partial t} = \epsilon h(\eta). \tag{2.15}$$

Notice this implies that $h(\eta) = T^*(\eta,\eta) - T_c$ where $T^*(\eta,\eta)$ is the equilibrium temperature at the ice line. We can substitute in $T^*(\eta,\eta)$ to see that for solutions to the Budyko-Widiasih model:

$$h(\eta) = \frac{Q}{B+C}\left(s(\eta)(1-\alpha(\eta,\eta)) + \frac{C}{B}(1-\overline{\alpha}(\eta))\right) - \frac{A}{B} - T_c. \tag{2.16}$$

The function h is used to approximate the behavior of the ice line η in system (2.10) over time . Since this derivation was independent of the chosen albedo function (although the result from [15] places certain restrictions on the albedo function), this equation can be solved numerically for any albedo function specified. The h function using the albedo function (2.4) is graphed using MATLAB in Figure 2.1. From this picture we can begin to understand the dynamics of the model. The ice line is at an equilibrium when $h(\eta) = 0$. Thus there are two equilibrium points: $\eta_1 \approx .95$ and $\eta_2 \approx .25$. Notice that when $h(\eta) > 0$, $\overline{T^*}(\eta,\eta) > T_c$ and thus the ice at the ice line will melt, resulting in an increasing η (and vice-versa). Thus we see that if $\eta \in (.25, 1]$, the ice line will converge over time to the equilibrium η_2. If $\eta \in [0, .25)$, the ice line will continue to grow until it reaches the boundary $\eta = 0$. Thus, since there is a region around the equilibrium point η_2 such that the long-term solutions converge to η_2, we would expect η_2 to be a stable equilibrium point. Since there is no region around the equilibrium point η_1 such that the long-term solutions converge to η_1, we would expect η_1 to be an unstable equilibrium point. Likewise, we would expect the boundary point $\eta = 0$ to be stable and $\eta = 1$ to be unstable. Thus this model gives two stable ice caps, one that corresponds to an ice cap like what we see today and one such that the entire Earth is covered by glaciers which corresponds to the Snowball Earth state. McGehee and Widiasih solve for an approximation to the model to show that these equilibrium points have the stability we would expect from the analysis above [8].

Notice that as stated this model follows the hypothesis of the Snowball Earth in that there is no condition for the thinning of the ice as it approaches the equator. Abbot et al. argue that when the ice line enters the area of the Earth's surface under which the Hadley cell circulation occurs, the Hadley cell zone, the evaporation exceeds the precipitation and thus the albedo of the glaciers below the ice line becomes the albedo of non-snow covered ice $\alpha_s > \alpha_i > \alpha_w$ [1]. Thus they instead use the albedo function

$$\alpha(y,\eta) = \begin{cases} \alpha_2(y), & y > \eta \\ \frac{1}{2}(\alpha_w + \alpha_2(\eta)), & y = \eta \\ \alpha_w, & y < \eta \end{cases} \tag{2.17}$$

where

$$\alpha_2(y) = \frac{1}{2}(\alpha_s + \alpha_i) + \frac{1}{2}(\alpha_s - \alpha_i)\tanh S(y-\rho), \tag{2.18}$$

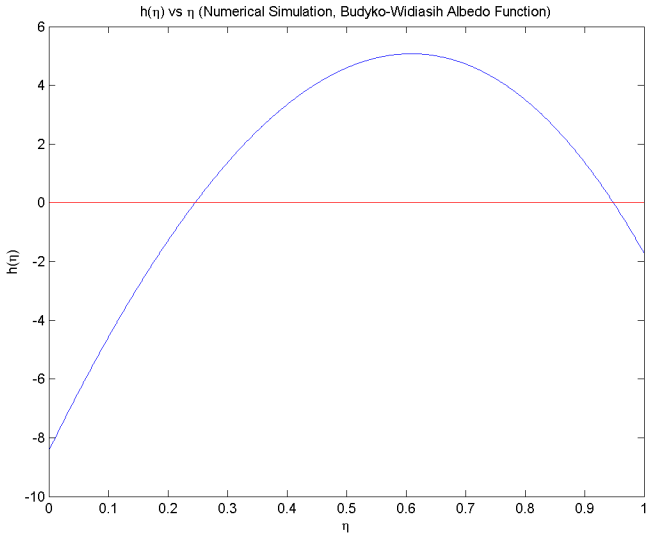

Figure 2.1: The h function for the Budyko-Widiasih Albedo Function .

$\eta < \rho$	$\eta > \rho$
$\alpha(y,\eta) = \begin{cases} \alpha_s, & y > \rho \\ \alpha_i, & \eta < y < \rho \\ \alpha_w, & y < \eta \end{cases}$	$\alpha(y,\eta) = \begin{cases} \alpha_s, & y > \eta \\ \alpha_w, & y < \eta \end{cases}$

Table 1: The Jormungand Instant Albedo Function

$\rho = .35$, a region under the descending branch of the Hadley circulation, $\alpha_i = .45$, and S is a constant. We can understand this albedo function by analogy to what we can call the Instant Jormungand Albedo Function,

Notice that this albedo function says that if the ice line is above the Hadley cell zone then the albedo function is the Budyko Albedo Function. However, if the ice-line falls below the latitude of furthest extent for the Hadley cell zone, then a third step in the albedo function is introduced where between η and ρ the ice is non-snow covered ice. Abbot's Albedo Function follows the same logic but instead uses a hyperbolic tangent function to do a continuous change between the middle and highest steps of the albedo function where the steepness of the change is controlled by the constant S (where increasing S increases the steepness of the change).

The parameter values are also adjusted in Abbot's model to account for the different atmospheric makeup that occurred during the Neoproterozoic era. These values are shown in Table 2. We can solve for the h function with Abbot's albedo function using equation (2.16). This was done numerically using MATLAB and is graphed in Figure 2.2. Doing the same analysis as before, we see that there should be two stable equilibrium points, $\eta_1 \approx .35$ and $\eta_3 \approx .95$, an unstable equilibrium point $\eta_2 \approx .70$, with the boundaries also unstable. The small stable ice cap is much like the ice cap from the Budyko-Widiasih model, however the

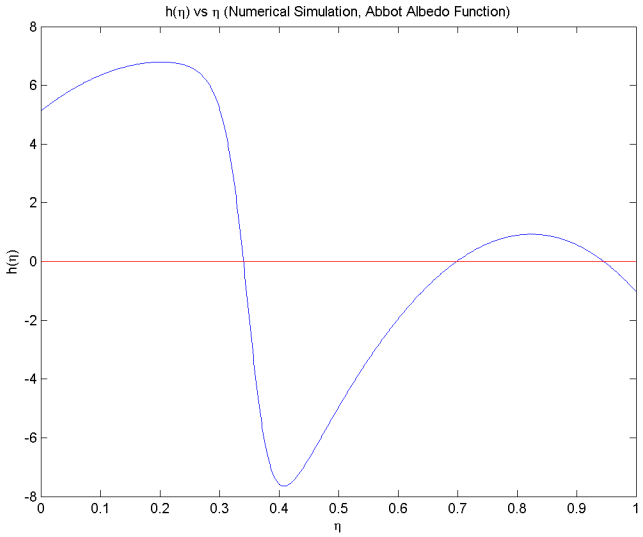

Figure 2.2: The h function for Abbot's Albedo Function.

Parameter	Value
Q	$321\,W/m^2$
A	$170\,W/m^2$
B	$1.5\,\frac{W/m^2}{^\circ C}$
C	$2.25\,\frac{W/m^2}{^\circ C}$
α_s	.8
α_w	.35

Table 2: Parameter values for Abbot's model.

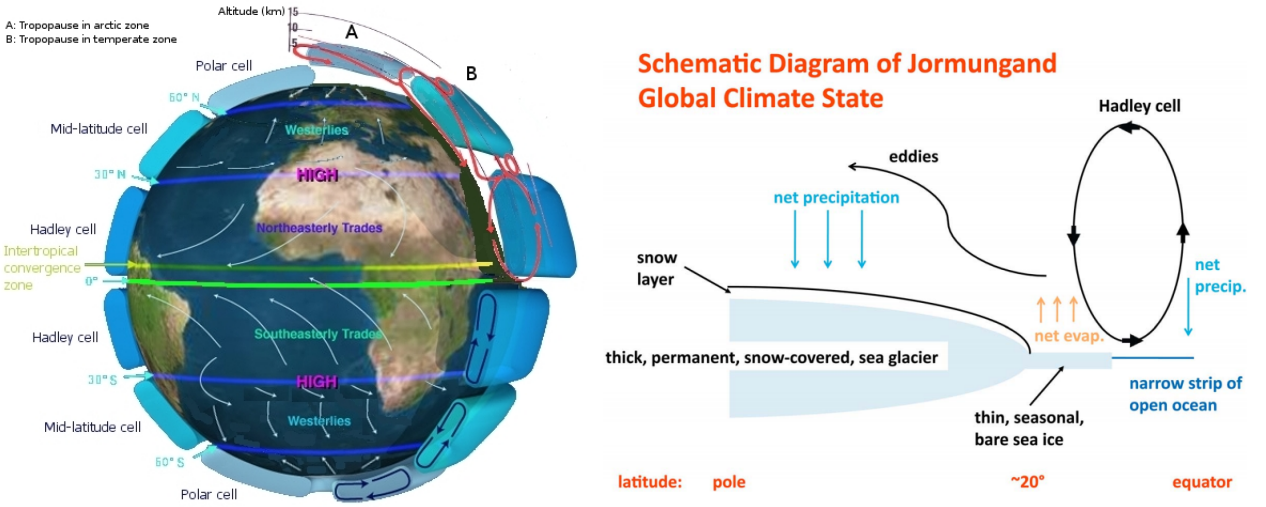

(a) A picture of the primary circulation cells [2].

(b) A diagram of the Hadley Cell's interaction with the ice line [1].

Figure 3.1: The Hadley Cells

stable large ice cap solution now includes a belt of open water and a small area where non-snow covered ice exists. Thus this stable large ice cap represents a Jormungand state. Abbot et al. analyze the strength of the hysteresis for the Jormungand state and concludes that this model shows the possibility of a Jormungand solution (further discussion on hysteresis analysis is presented in Section 3.3.4).

3 The Budyko-Widiasih Model with the Linear Jormungand Albedo Function

3.1 More Information on the Hadley Cells

The driving force that causes the bare sea ice in Abbot's albedo function are the Hadley cells. The Hadley cells are one of the Earth's three primary circulation cells and the closest primary circulation cell to the equator. It is depicted in Figure 3.1a. It spans from the equator to about $30°N$ [14], though its range is dependent on many factors [7]. Abbot et al. found in general circulation models that the furthest extent of the Hadley cells in a condition that gave rise to a stable Jormungand state was $20°N$, or $\rho \approx .35$. The Hadley cells cause well-known effects such as trade winds, tropical rain-belts, hurricanes, subtropical deserts (such as the Sahara Desert), and jet streams. The purpose for the introduction of the Hadley cells into the model is the effect on subtropical precipitation and evaporation depicted in Figure 3.1b. Notice that as the air gets closer to the equator it begins to warm up. This warming causes the air to rise and decrease in pressure. This decrease in pressure decreases the air's ability to hold water vapor and as a result there is a net precipitation near the equator. When the air falls at the furthest edges of the Hadley Cell zone, it has a low water vapor concentration which causes a net evaporation.

Abbot et al. show the existence of this effect using simulations with general circulation models. Figure 3.2a shows that in the ice-free state there is a net evaporation at most latitudes in the Hadley cell zone and the same (but decreased effect) is seen in the Jormungand state. This suggests that during the onset of a

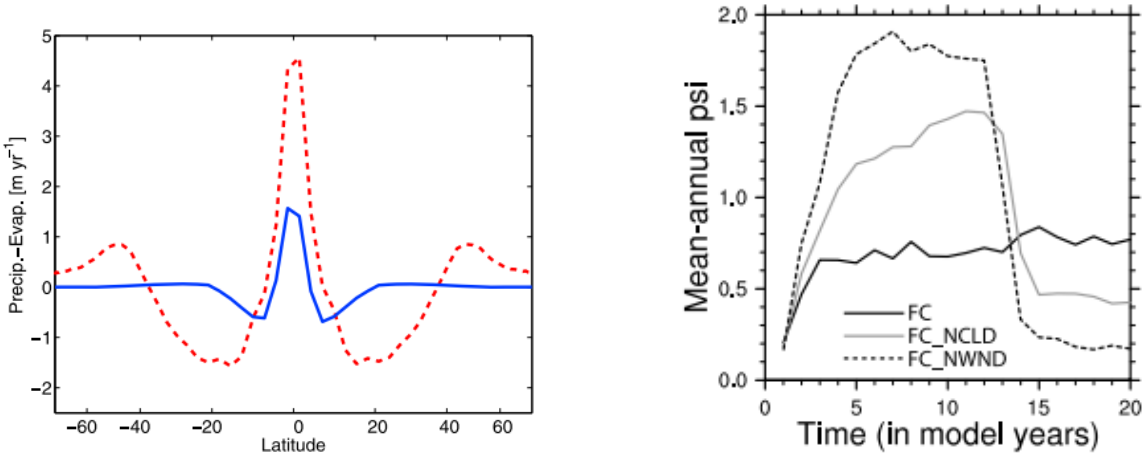

(a) Annual and zonal mean precipitation minus evaporation for the ice-free state (red dashed) and the Jormungand state (blue) with $pCO_2 = 5000$ ppm [1].

(b) Maximum intensity of the Hadley cells circulation. The different lines indicate different processes turned on/off. These show an intensification of the Hadley cells as the sea ice advances into lower latitudes and an abrupt weakening just prior to complete freezing. Some simulations result in an instant intensification while others result in a more gradual intensification. [12] .

Figure 3.2: Global climate model results for Hadley Cell dynamics.

Jormungand state (as the ice line approaches the stable Jormungand condition) there is a net evaporation over much of the Hadley cell zone. Additionally Paulson and Jacob examined the intensity of the Hadley cells circulation at the onset of Snowball Earth in general circulation models [12]. They found that as the Earth's state approaches Snowball Earth the Hadley cells intensify as shown in Figure 3.2b.

3.2 The Linear Jormungand Albedo Function

These results show that as the ice line enters the Hadley cell zone the albedo becomes closer to that of bare sea ice due to a net evaporation. However, since we are looking at the annual averages, this does not imply that the albedo of the glaciers in the Hadley cell zone instantly becomes α_i. An example to help one understand this is to know that Tuscon, Arizona, a place with a net evaporation (i.e. a desert), received a freak snow storm in the winter of 2013. However, being a desert with a high net evaporation, the snow evaporated quickly and was gone in less than a day. Thus even though there is a net evaporation for a given year, the ice sheets would still be covered in snow at various times in the year. As the Hadley cells ramp up, there would be a larger net evaporation in most of the Hadley cell area and thus we would expect the albedo of the ice in the Hadley cell zone to fall closer to α_i.

When the ice is at the edge of the Hadley cell zone $\eta = \rho$ the albedo of the ice in the Hadley cell zone should be close to α_s and as the ice line approaches the equator the Hadley cell should be in full force making the albedo of the ice in the Hadley cell zone close to α_i. We can approximate this process linearly with the Linear Jormungand Albedo Function shown in Table 3.

Pictures of the Linear Jormungand Albedo Function displayed as Figure 3.3.

$\eta < \rho$	$\eta > \rho$
$\alpha(y,\eta) = \begin{cases} \alpha_s, & y > \rho \\ \alpha_b(\eta), & \eta < y < \rho \\ \alpha_w, & y < \eta \end{cases}$	$\alpha(y,\eta) = \begin{cases} \alpha_s, & y > \eta \\ \alpha_w, & y < \eta \end{cases}$

$$\alpha_b(\eta) = \frac{\alpha_s - \alpha_i}{\rho}\eta + \alpha_i. \tag{3.1}$$

Table 3: The Jormungand Linear Albedo Function.

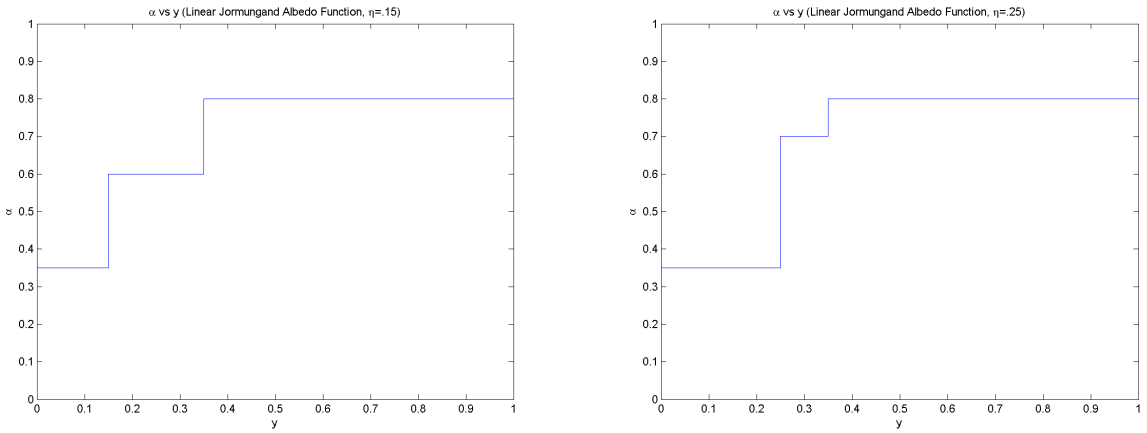

(a) $\eta = .15$ (b) $\eta = .25$

Figure 3.3: Linear Jormungand Albedo Function graphs.

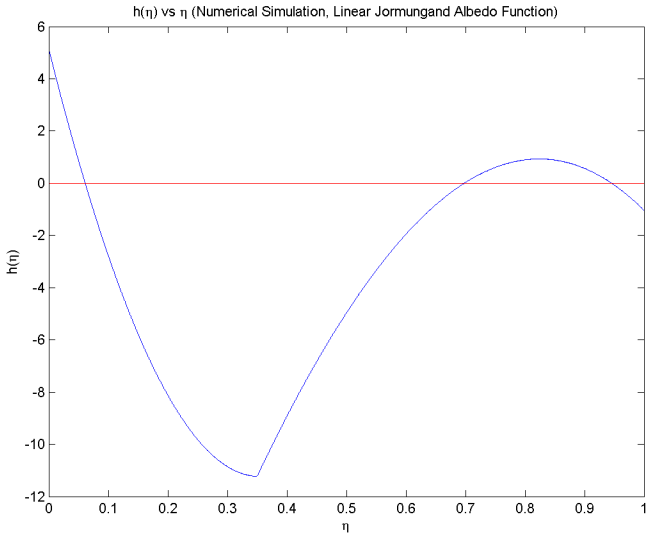

Figure 3.4: The h function for the Linear Jormungand Albedo Function.

$\eta < \rho$	$\eta > \rho$
$\alpha(y,\eta) = \begin{cases} \alpha_s, & y > \rho \\ \alpha_b(\eta), & \eta < y < \rho \\ \alpha_w, & y < \eta \end{cases}$	$\alpha(y,\eta) = \begin{cases} \alpha_s, & y > \eta \\ \alpha_w, & y < \eta \end{cases}$

Table 4: The general albedo function.

We can solve for h using equation (2.16). This was done numerically using MATLAB and can be seen in Figure 3.4. Using the analysis from before, this graph suggests that there should be two stable equilibrium points, $\eta_1 \approx .1$ and $\eta_3 \approx .95$, an unstable equilibrium point, $\eta_2 \approx .7$, and the boundaries are unstable. The large stable ice cap η_1 corresponds to a Jormungand state like the one from Figure 2.2, however in this model it is much closer to the equator. The reason it is closer to the equator is because $\alpha_b > \alpha_i$ for $\eta > 0$ and thus with a larger albedo we would expect a colder overall climate which results in a solution that stabilizes closer to the equator.

3.3 Analytical Approximation

In order to verify the existence and stability of the large ice cap solution we will solve for an analytical approximation to the h function. We will solve for the function h piecewise for the more general albedo function depicted in Table 4 where $\alpha_b(\eta) \in C^\infty$. When $\eta > \rho$ the albedo function is equivalent to the Budyko albedo function (2.4). Previous research solved for an approximation to the h function for the Budyko albedo function [8]. Thus our focus is on the case where $\eta < \rho$.

When $\eta < \rho$, the albedo function is the three step function

$$\alpha(y,\eta) = \begin{cases} \alpha_s, & y > \rho \\ \alpha_b(\eta), & \eta < y < \rho \\ \alpha_w, & y < \eta \end{cases} \tag{3.2}$$

We can write

$$T(y,t) = \begin{cases} U(y,t), & y < \eta \\ V(y,t), & \eta < y < \rho \\ W(y,t), & y \geq \rho \\ \frac{1}{2}(U(\eta,t) + V(\eta,t)), & y = \eta. \end{cases} . \tag{3.3}$$

Thus our equations become

$$\begin{aligned} R\frac{\partial U}{\partial t} &= Qs(y)(1-\alpha_s) - (A + BU) - C(U - \overline{T}), \\ R\frac{\partial V}{\partial t} &= Qs(y)(1-\alpha_b(\eta)) - (A + BV) - C(V - \overline{T}), \\ R\frac{\partial W}{\partial t} &= Qs(y)(1-\alpha_w) - (A + BW) - C(W - \overline{T}), \\ \frac{\partial \eta}{\partial t} &= \epsilon(T(\eta,\eta) - T_c). \end{aligned} \tag{3.4}$$

3.3.1 Legendre Expansion

Since the insolation distribution function s is quadratic in y, we will assume that the temperature distribution functions U, V, and W are quadratic in y. Since the model is symmetric about $y = 0$, we will assume that U, V, and W are even functions. We can write these functions using the Legendre polynomials. The Legendre polynomials form an orthogonal basis for the set of polynomial functions. Denote $p_i(y)$ to be the i^{th} order Legendre polynomial. Any polynomial function $f(y)$ can be written as

$$f(y) = c_0 p_o(y) + c_1 p_1(y) + \dots \tag{3.5}$$

The reason such an expansion can be more helpful than a Taylor series expansion is due to the orthogonality property

$$\int_0^1 p_i(y) p_j(y) dy = 0 \tag{3.6}$$

for $i \neq j$ and that these polynomials satisfy the eigenvalue equation for the diffusion equation which is often used in such models. Since our function is quadratic and even, our expansion requires only the first two even Legendre polynomials

$$\begin{aligned} p_0(y) &= 1, \\ p_2(y) &= \frac{1}{2}(3y^2 - 1). \end{aligned} \tag{3.7}$$

Thus we can write

$$\begin{aligned} U(y,t) &= u_0(t)p_0(y) + u_2(t)p_2(y), \\ V(y,t) &= v_0(t)p_0(y) + v_2(t)p_2(y), \\ W(y,t) &= w_0(t)p_0(y) + w_2(t)p_2(y). \end{aligned} \tag{3.8}$$

For the simplicity of further calculations and formulas, define the equations

$$\begin{aligned} P_0(x) &= \int_0^x p_0(y)dy = x, \\ P_2(x) &= \int_0^x p_2(y)dy = \frac{1}{2}(x^3 - x). \end{aligned} \tag{3.9}$$

Notice that by solving for the Legendre expansion coefficients one solves for the temperature distribution functions themselves. Thus we wish to write the model in terms of these Legendre expansion coefficients. First, notice that

$$T(\eta,\eta) = \frac{1}{2}(U(\eta,t) + V(\eta,t)) = \frac{1}{2}(u_0 + v_0) + \frac{1}{2}(u_2 + v_2)p_2(\eta). \tag{3.10}$$

Now we will rewrite the global average annual temperature in terms of the Legendre coefficients

$$\begin{aligned} \overline{T}(\eta) &= \int_0^\eta U(y,t)dy + \int_\eta^\rho V(y,t)dy + \int_\rho^1 W(y,t)dy, \\ &= \int_0^\eta (u_0p_0 + u_2p_2)dy + \int_\eta^\rho (v_0p_0 + v_2p_2)dy + \int_\rho^1 (w_0p_0 + w_2p_2)dy, \\ &= u_0P_0(\eta) + u_2P_2(\eta) + v_0(P_0(\rho) - P_0(\eta)) + v_2(P_2(\rho) - P_2(\eta)) + w_0(P_0(1) - P_0(\rho)) + w_2(P_2(1) - P_2(\rho)), \\ &= u_0\eta + u_2P_2(\eta) + v_0(P_0(\rho) - P_0(\eta)) + v_2(P_2(\rho) - P_2(\eta)) + w_0(1 - \rho) + w_2P_2(\rho). \end{aligned}$$

We wish to rewrite s in its Legendre expansion

$$s(y) = 1.241 - .0723y^2 = s_0p_0(y) + s_2p_2(y). \tag{3.11}$$

Notice that due to the normality of s,

$$\int_0^1 s(y)dy = 1 = \int_0^1 (s_0p_0(y) + s_2p_2(y))dy = s_0P_0(1) + s_2P_2(1) = s_0 \tag{3.12}$$

and thus $s_0 = 1$. Therefore we see that to receive the right constant term for s, $-\frac{1}{2}s_2 + 1 = 1.241$ which implies $s_2 = -.482$. Remembering $p_0 = 1$, we can write out our equations as

$$\begin{aligned} \dot{u}_0p_0 + \dot{u}_2p_2 &= \frac{1}{R}(Q(p_0 + s_2p_2)(1 - \alpha_s) - Ap_0 + B(u_0p_0 + u_2p_2) - C(u_0p_0 + u_2p_2) - C\overline{T}p_0), \\ \dot{v}_0p_0 + \dot{v}_2p_2 &= \frac{1}{R}(Q(p_0 + s_2p_2)(1 - \alpha_b(\eta)) - Ap_0 + B(v_0p_0 + v_2p_2) - C(v_0p_0 + v_2p_2) - C\overline{T}p_0), \\ \dot{w}_0p_0 + \dot{w}_2p_2 &= \frac{1}{R}(Q(p_0 + s_2p_2)(1 - \alpha_w) - Ap_0 + B(w_0p_0 + w_2p_2) - C(w_0p_0 + w_2p_2) - C\overline{T}p_0), \end{aligned}$$

where $\dot{f}$ means the time derivative of f. We can expand out these equations and write them in the form

$$\dot{f}_0p_0 + \dot{f}_2p_2 = c_0p_0 + c_2p_2 \tag{3.13}$$

from which it follows

$$\begin{aligned} \dot{f}_0 &= c_0, \\ \dot{f}_2 &= c_2. \end{aligned} \tag{3.14}$$

Thus we can rewrite our model in the following form:

$$\begin{aligned} \dot{\eta} &= \epsilon(T(\eta,\eta) - T_c), \\ \dot{u}_0 &= \frac{1}{R}(Q(1-\alpha_w) - A - (B+C)u_0 + C\overline{T}(\eta)), \\ \dot{v}_0 &= \frac{1}{R}(Q(1-\alpha_b(\eta)) - A - (B+C)v_0 + C\overline{T}(\eta)), \\ \dot{w}_0 &= \frac{1}{R}(Q(1-\alpha_s) - A - (B+C)w_0 + C\overline{T}(\eta)), \\ \dot{u}_2 &= \frac{1}{R}(Qs_2(1-\alpha_w) - (B+C)u_2), \\ \dot{v}_2 &= \frac{1}{R}(Qs_2(1-\alpha_b(\eta)) - (B+C)v_2), \\ \dot{w}_2 &= \frac{1}{R}(Qs_2(1-\alpha_s) - (B+C)w_2). \end{aligned} \tag{3.15}$$

where

$$\begin{aligned} T(\eta,\eta) &= \frac{1}{2}(u_0+v_0) + \frac{1}{2}(u_2+v_2)p_2(\eta), \\ \overline{T}(\eta) &= u_0\eta + u_2P_2(\eta) + v_0(P_0(\rho) - P_0(\eta)) + v_2(P_2(\rho) - P_2(\eta)) + w_0(1-\rho) + w_2P_2(\rho). \end{aligned} \tag{3.16}$$

3.3.2 Substitutions

Notice that the equations for u_2 and w_2 are simple linear equations that are decoupled from the other variables. Therefore we can solve these equations independently from the rest of the system. If $u_2 > \frac{Qs_2(1-\alpha_w)}{B+C}$ then $\dot{u}_2 < 0$ and that if $u_2 < \frac{Qs_2(1-\alpha_w)}{B+C}$ then $\dot{u}_2 > 0$. Thus as $t \to \infty$, $u_2 \to \frac{Qs_2(1-\alpha_w)}{B+C}$. The same reasoning shows $w_2 \to \frac{Qs_2(1-\alpha_s)}{B+C}$ as $t \to \infty$. Thus we have reduced the number of variables in our model to make our system

$$\begin{aligned} \dot{\eta} &= \epsilon(T(\eta,\eta) - T_c), \\ \dot{u}_0 &= \frac{1}{R}(Q(1-\alpha_w) - A - (B+C)u_0 + C\overline{T}(\eta)), \\ \dot{v}_0 &= \frac{1}{R}(Q(1-\alpha_b(\eta)) - A - (B+C)v_0 + C\overline{T}(\eta)), \\ \dot{w}_0 &= \frac{1}{R}(Q(1-\alpha_s) - A - (B+C)w_0 + C\overline{T}(\eta)), \\ \dot{v}_2 &= \frac{1}{R}(Qs_2(1-\alpha_b(\eta)) - (B+C)v_2), \end{aligned} \tag{3.17}$$

What we wish to do is find substitutions to further reduce the dimensionality of the model in a similar manner.

First Substitution: Let $x = \frac{1}{2}(u_0 + v_0)$, $z = u_0 - v_0$. The system becomes

$$\begin{aligned}
\dot{\eta} &= \epsilon(T(\eta,\eta) - T_c), \\
\dot{x} &= \frac{1}{R}(Q(1 - \frac{1}{2}(\alpha_w + \alpha_b(\eta))) - A - (B+C)x + C\overline{T}(\eta)), \\
\dot{z} &= \frac{1}{R}(Q(\alpha_b(\eta) - \alpha_w) - (B+C)z), \\
\dot{w}_0 &= \frac{1}{R}(Q(1-\alpha_s) - A - (B+C)w_0 + C\overline{T}(\eta)), \\
\dot{v}_2 &= \frac{1}{R}(Qs_2(1-\alpha_b(\eta)) - (B+C)v_2),
\end{aligned} \tag{3.18}$$

where

$$\begin{aligned}
T(\eta,\eta) &= x + \frac{1}{2}(u_2 + v_2)p_2(\eta), \\
\overline{T}(\eta) &= (\eta - \frac{\rho}{2})z + \rho x + u_2 P_2(\eta) - v_2(P_2(\eta) - P_2(\rho)) + (1-\rho)w_0 - P_2(\rho)w_2.
\end{aligned} \tag{3.19}$$

Second Substitution: Let $a = \frac{1}{2}(x + w_0)$, $b = x - w_0$. The system becomes

$$\begin{aligned}
\dot{\eta} &= \epsilon(T(\eta,\eta) - T_c), \\
\dot{a} &= \frac{1}{R}(Q(1 - \frac{1}{2}(\alpha_s + \frac{1}{2}(\alpha_w + \alpha_b(\eta)))) - A - (B+C)a + C\overline{T}(\eta)), \\
\dot{b} &= \frac{1}{R}(Q(\alpha_s - \frac{1}{2}(\alpha_w + \alpha_b(\eta))) - (B+C)b), \\
\dot{z} &= \frac{1}{R}(Q(\alpha_b(\eta) - \alpha_w) - (B+C)z), \\
\dot{v}_2 &= \frac{1}{R}(Qs_2(1-\alpha_b(\eta)) - (B+C)v_2),
\end{aligned} \tag{3.20}$$

where

$$\begin{aligned}
T(\eta,\eta) &= a + \frac{b}{2} + \frac{1}{2}(u_2 + v_2)p_2(\eta), \\
\overline{T}(\eta) &= (\eta - \frac{\rho}{2})z + u_2 P_2(\eta) - v_2(P_2(\eta) - P_2(\rho)) + a + b(\rho - \frac{1}{2}) - P_2(\rho)w_2.
\end{aligned} \tag{3.21}$$

Third Substitution: $d = s_2 z + v_2$. The system becomes

$$\begin{aligned}
\dot{\eta} &= \epsilon(T(\eta,\eta) - T_c), \\
\dot{a} &= \frac{1}{R}(Q(1 - \frac{1}{2}(\alpha_s + \frac{1}{2}(\alpha_w + \alpha_b(\eta)))) - A - (B+C)a + C\overline{T}(\eta)), \\
\dot{b} &= \frac{1}{R}(Q(\alpha_s - \frac{1}{2}(\alpha_w + \alpha_b(\eta))) - (B+C)b), \\
\dot{z} &= \frac{1}{R}(Q(\alpha_b(\eta) - \alpha_w) - (B+C)z), \\
\dot{d} &= \frac{1}{R}(Qs_2(1-\alpha_w) - (B+C)d),
\end{aligned} \tag{3.22}$$

where

$$\begin{aligned} T(\eta,\eta) &= a+\frac{b}{2}+\frac{1}{2}(u_2+d-s_2z)p_2(\eta), \\ \overline{T}(\eta) &= (\eta-\frac{\rho}{2}+s_2(P_2(\eta)-P_2(\rho)))z+u_2P_2(\eta)-d(P_2(\eta)-P_2(\rho))+a+b(\rho-\frac{1}{2})-P_2(\rho)w_2. \end{aligned} \tag{3.23}$$

Notice d is decoupled from the rest of the system variables and thus

$$d \to \frac{Qs_2(1-\alpha_w)}{B+C} \text{ as } t \to \infty. \tag{3.24}$$

Fourth Substitution: $e = 2b + z$. The system becomes

$$\begin{aligned} \dot{\eta} &= \epsilon(T(\eta,\eta)-T_c), \\ \dot{a} &= \frac{1}{R}(Q(1-\frac{1}{2}(\alpha_s+\frac{1}{2}(\alpha_w+\alpha_b(\eta))))-A-(B+C)a+C\overline{T}(\eta)), \\ \dot{e} &= \frac{1}{R}(2Q(\alpha_s-\alpha_w))-(B+C)e), \\ \dot{z} &= \frac{1}{R}(Q(\alpha_b(\eta)-\alpha_w)-(B+C)z), \end{aligned} \tag{3.25}$$

where

$$\begin{aligned} T(\eta,\eta) &= a+\frac{1}{4}(e-z)+\frac{1}{2}(u_2+d-s_2z)p_2(\eta), \\ \overline{T}(\eta) &= (\eta-\rho+\frac{1}{4}+s_2(P_2(\eta)-P_2(\rho)))z+u_2P_2(\eta)-d(P_2(\eta)-P_2(\rho))+a+\frac{1}{2}e(\rho-\frac{1}{2})-P_2(\rho)w_2. \end{aligned} \tag{3.26}$$

Notice e is decoupled from the rest of the system variables making

$$e = \frac{2Q(\alpha_s-\alpha_w)}{B+C} \text{ as } t \to \infty. \tag{3.27}$$

making our system

$$\begin{aligned} \dot{\eta} &= \epsilon(T(\eta,\eta)-T_c), \\ \dot{a} &= \frac{1}{R}(Q(1-\frac{1}{2}(\alpha_s+\frac{1}{2}(\alpha_w+\alpha_b(\eta))))-A-(B+C)a+C\overline{T}(\eta)), \\ \dot{z} &= \frac{1}{R}(Q(\alpha_b(\eta)-\alpha_w)-(B+C)z). \end{aligned} \tag{3.28}$$

3.3.3 Geometric Singular Perturbation Theory Approximation

McGehee and Widiasih estimated that $\epsilon \approx 3.9 \times 10^{-13}$ [8]. Thus the changes in η for a given change in time are much smaller than those for the other variables. Therefore we denote η as the slow variable and a and z as the fast variables. We will use the theorems from geometric singular perturbation theory to understand the solution to the model [5].

We can write our system as

$$\begin{aligned} \dot{X} &= f(X,Y,\epsilon), \\ \dot{Y} &= \epsilon g(X,Y,\epsilon), \end{aligned} \tag{3.29}$$

where X is the vector of the fast variables (a, z) and Y is the vector of the slow variables (η). Alternatively, we can rewrite the equation in the slow time frame $\tau = \epsilon t$ to get

$$\begin{aligned} \epsilon \dot{X} &= f(X, Y, \epsilon), \\ \dot{Y} &= g(X, Y, \epsilon). \end{aligned} \tag{3.30}$$

Notice that since $\dot{\eta}$, $\dot{a}$, and $\dot{z}$ are polynomials in the variables and $\alpha_b(\eta) \in C^\infty$, it follows that $f, g \in C^\infty$. Let M_0 be any compact subset of $\{(X, Y) : f(X, Y, 0) = 0\}$, the manifold defined by parameters that satisfy the model when $\epsilon = 0$. We can write the manifold

$$M_0 = \{(X, Y) : X = h^0(Y)\} \tag{3.31}$$

where $h^0(Y)$ is defined for $Y \in K$, a compact domain of $\mathbb{R}$. Fenichel's Theorems assert that there exists a manifold M_ϵ that lies $\mathcal{O}(\epsilon)$ from M_0 and is diffeomorphic to M_0 [5]. Moreover, it is locally invariant under the flow defined by our system. Thus we can write

$$M_\epsilon = \{(X, Y) : X = h^\epsilon(Y)\}, \tag{3.32}$$

where

$$h^\epsilon(Y) = h^0(Y) + \mathcal{O}(\epsilon). \tag{3.33}$$

The big result is that in the flow of the slow variables on the M_ϵ manifold can be written in the slow time scale as

$$\dot{Y} = g(h^\epsilon(Y), Y, \epsilon) = g(h^0(Y), Y, 0) + \mathcal{O}(\epsilon). \tag{3.34}$$

This means that the flows of the slow variables are well-approximated by the flow on the M_0 manifold.

Since Y is simply the vector with the variable η, $g(h^\epsilon(Y), Y, \epsilon)$ is the function that we called in earlier sections h. To find this function h, we need to first solve for the manifold M_0 and the graph of the parameters on this manifold $h^0(\eta)$. Recall that M_0 is the manifold where $f(X, Y, 0) = 0$, and thus it corresponds to the points which satisfy what is known as the Fast Subsystem, the fast time system where $\epsilon = 0$:

$$\begin{aligned} \dot{\eta} &= 0, \\ \dot{a} &= \frac{1}{R}(Q(1 - \frac{1}{2}(\alpha_s + \frac{1}{2}(\alpha_w + \alpha_b(\eta)))) - A - (B + C)a + C\overline{T}(\eta)), \\ \dot{z} &= \frac{1}{R}(Q(\alpha_b(\eta) - \alpha_w) - (B + C)z). \end{aligned} \tag{3.35}$$

Since $\dot{\eta} = 0$, we can treat η as a parameter and thus we see that over time a and z will converge to values that are functions of η. Thus M_0 is the manifold defined by the set of points that satisfy

$$\begin{aligned} a^0(\eta) &= \frac{Q(1 - \frac{1}{2}(\alpha_s + \frac{1}{2}(\alpha_w + \alpha_b(\eta)))) - A + C\psi(\eta)}{B}, \\ z^0(\eta) &= \frac{Q(\alpha_b(\eta) - \alpha_w)}{B + C}, \end{aligned} \tag{3.36}$$

where

$$\psi(\eta) = \overline{T}(\eta) - a. \tag{3.37}$$

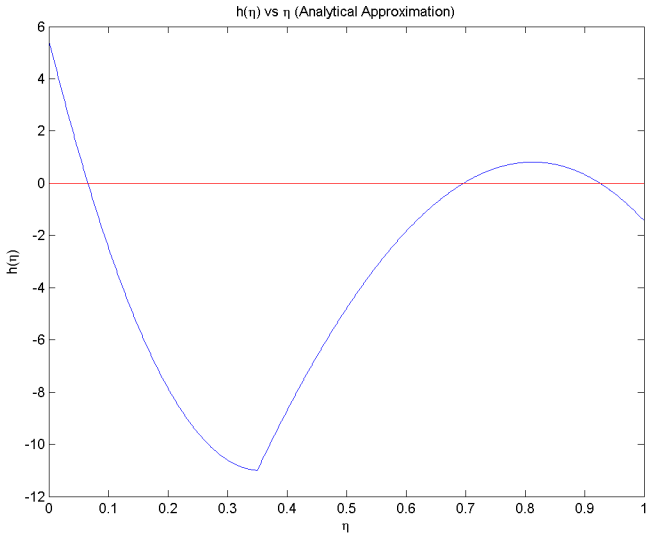

Figure 3.5: The analytical approximation to the h function for the Linear Jormungand Albedo Function.

Thus we have solved for $h^0(\eta) = (a^0(\eta), z^0(\eta))$. Since

$$g(h^\epsilon(Y), Y, \epsilon) = T(\eta, \eta) - T_c, \tag{3.38}$$

we see that $g(h^0(Y), Y, 0)$ is simply the function where we plug in $a^0(\eta)$ and $z^0(\eta)$ for a and z respectively in $T(\eta, \eta) - T_c$, and thus

$$g(h^0(Y), Y, 0) = a^0(\eta) + \frac{1}{4}(e - z^0(\eta)) + \frac{1}{2}(u_2 + d - s_2 z)p_2(\eta). \tag{3.39}$$

Therefore we can solve for the function h as

$$h(\eta) = g(h^\epsilon(Y), Y, \epsilon) = g(h^0(Y), Y, 0) + \mathcal{O}(\epsilon) \approx a^0(\eta) + \frac{1}{4}(e - z^0(\eta)) + \frac{1}{2}(u_2 + d - s_2 z)p_2(\eta). \tag{3.40}$$

Putting together this solution piecewise from the solution for $\eta > \rho$ from McGehee-Widiasih [8] we can graph our approximation to h as seen in Figure 3.5. Notice that this solution looks virtually identical to Figure 3.4 and thus the function h is well-approximated by the function found by this approximation.

3.3.4 Stability and Hysteresis

We wish to understand the stability and the hysteresis associated with the large ice cap equilibrium. To understand the stability of the equilibrium, we must look at the eigenvalues of the Jacobin matrix

$$\begin{pmatrix} \frac{\partial \dot{\eta}}{\partial \eta} & \frac{\partial \dot{\eta}}{\partial a} & \frac{\partial \dot{\eta}}{\partial z} \\ \frac{\partial \dot{a}}{\partial \eta} & \frac{\partial \dot{a}}{\partial a} & \frac{\partial \dot{a}}{\partial z} \\ \frac{\partial \dot{z}}{\partial \eta} & \frac{\partial \dot{z}}{\partial a} & \frac{\partial \dot{z}}{\partial z} \end{pmatrix}. \tag{3.41}$$

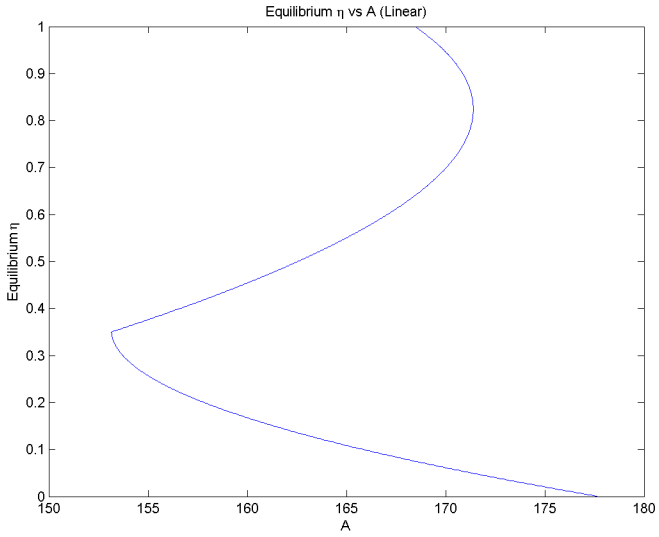

Figure 3.6: Bifurcation plot for the parameter A for the Linear Jormungand model.

This was done in Mathematica and for the equilibrium point $\eta \approx .1$ the eigenvalues are -3.75, -1.5, and -3×10^{-11}. Since all of the eigenvalues are negative, by the Hartman-Grobman Theorem the equilibrium at $\eta \approx .1$ is stable.

Recall that A is a constant which corresponds to the amount of energy that leaves the Earth's system. Increasing A results in increases in the energy that is released from the Earth's system and thus acts in the same manner as a decrease in the CO_2 content of the atmosphere. We can understand the hysteresis of CO_2, the range of CO_2 concentrations where both the Jormungand and the small ice cap states are stable, by plotting the bifurcation diagram of the equilibrium η vs A as shown in Figure 3.6. Thus we see that there is a large range of A, from around $A \approx 153$ to $A \approx 171$, such that two stable states exist. This shows the strong hysteresis of the Linear Jormungand model.

4 Conclusions

The geological record indicates that there have been times where glaciers have grown near the equator, though as of yet we do not fully understand the nature of these glaciations. The Snowball Earth Hypothesis states that the Earth was covered entirely by glaciers. However, it is hard for this hypothesis to account for some biological evidence such as the survival of photosynthetic eukaryotes. Thus the Jormungand Hypothesis was developed as an alternative. We have altered the albedo function for the Budyko-Widiasih model to match the thin-ice claims of the Jormungand model in a way that corresponds to the Hadley Cell dynamics. The resultant model gives a stable equilibrium point of $\eta \approx .1$ which we take to be the Jormungand state.

References

[1] Abbot, Dorian S., Aiko Voigt, and Daniel Koll. The Jormungand Global Climate State and Implications for Neoproterozoic Glaciations. *Journal of Geophysical Research* 116.D18 (2011). Print.

[2] Hadley Cell. Wikipedia. *Wikimedia Foundation*, 29 Mar. 2013.

[3] Hoffman, Paul F., Alan J. Kaufman, Galen P. Halverson, and Daniel P. Schrag. A Neoproterozoic Snowball Earth. *Science* 281 (1998): 1342-346. Print.

[4] Hoffman, Paul F., and Daniel P. Schrag. Snowball Earth. *Scientific American* Jan. 2000. Print.

[5] Jones, Christopher. Geometric Singular Perturbation Theory. *Dynamical Systems: Lectures given at the 2nd Session of the Centro Internazionale Matematico Estivo (C.I.M.E.) Held in Montecatini Terme, Italy*, June 13-22, 1994. Ed. Russel Johnson. Vol. 1609. Berlin: Springer, 1995. 44-118. Print.

[6] Kaper, Hans. Climate Modeling: Zonal Energy Balance Models. *2013 Joint Mathematics Meetings.* MAA Short Course on Climate Models, San Diego. 7 Jan. 2013. Lecture.

[7] Lu, Jian, Gabriel Vecchi, and Thomas Reichler. Expansion of the Hadley Cell under Global Warming. *Geophysical Research Letters* 34.L06805 (2007). Print.

[8] McGehee, Richard, and Esther Widiasih. A Simplification of Budyko's Ice-albedo Feedback Model. Preprint.

[9] McGehee, Richard, and James Walsh. Modeling Climate Dynamically. Preprint.

[10] Nave, Carl R. Magnetic Field of the Earth. Magnetic Field of the Earth. *Hyper Physics.* Web. 28 Mar. 2013.

[11] Perko, Lawrence. *Differential Equations and Dynamical Systems.* New York: Springer, 2001. Print.

[12] Poulsen, C. J., and R. L. Jacob. Factors That Inhibit Snowball Earth Simulation. *Paleoceanography* 19.PA4021 (2004). Print.

[13] Gerald R. North. Analytical solution to a simple climate model with diusive heat transport. *Journal of the Atmospheric Sciences*, 32:1301-1307, 1975.

[14] Pierrehumbert, Raymond T. *Principles of Planetary Climate.* Cambridge: Cambridge UP, 2010. Print.

[15] Widiasih, Esther. The Unstability of the Ice Free Earth: A Note on the Dynamics of One Dimensional Energy Balance Model. Preprint.